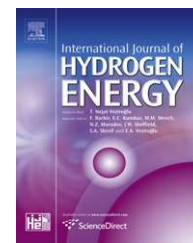


Available online at www.sciencedirect.com

SciVerse ScienceDirect

journal homepage: www.elsevier.com/locate/he

Numerical evaluation of internal combustion spark ignition engines performance fuelled with hydrogen – Natural gas blends

Antonio Mariani, Biagio Morrone*, Andrea Unich

Dipartimento di Ingegneria Aerospaziale e Meccanica, Seconda Università degli Studi di Napoli, via Roma 29, 81031 Aversa (CE), Italy

ARTICLE INFO

Article history:

Received 1 August 2011

Received in revised form

17 October 2011

Accepted 18 October 2011

Available online 2 December 2011

Keywords:

Hydrogen

Natural gas

Internal combustion engine

Fuel consumption

Exhaust gas recirculation

ABSTRACT

The dependence of road transportation from fossil fuels and the related economic and environmental consequences imposes the diversification of energy sources. Hydrogen can strongly contribute to this goal because it can be produced from different renewable energy sources.

In order to boost the development of hydrogen technology and reduce the dependence from conventional fossil fuels, hydrogen can be used in internal combustion engines added to natural gas (NG). Hydrogen-natural gas blends, commonly named HCNG, can be distributed using the natural gas infrastructures without significant modifications if hydrogen content is lower than 30% in volume.

In this paper a numerical model has been developed to predict the performance and emissions of an internal combustion engine fuelled by natural gas and hydrogen – natural gas blends. The analysis displayed the impact of hydrogen addition on engine brake efficiency and NO_x emission. Stoichiometric air-to-fuel ratio was considered for each fuel in order to assure an efficient exhaust after-treatment adopting a three-way catalyst. Exhaust gas recirculation (EGR) was investigated with the aim at improving engine efficiency and reducing NO_x emissions respect to undiluted charge. In fact, HCNG blends combustion properties are particularly suitable for EGR, assuring a stable combustion also when the charge is diluted. Maximum brake torque (MBT) ignition timing has been adopted for all fuels and operating conditions investigated.

Simulations were performed at conditions reproducing engine operation on a passenger car over the New European Driving Cycle (NEDC). Results were displayed in terms of fuel consumption in MJ/km and NO_x emissions in g/km.

The results showed that HCNG blends improved engine brake efficiency, particularly at low loads and for the highest hydrogen content, with fuel consumptions on energy basis over NEDC 2.5%, 4.7% and 5.7% lower than CNG, for HCNG 10, 20 and 30 respectively. NO_x emissions increased of about 4% for HCNG 10, 11% for HCNG 20 and 20% for HCNG 30, due to the higher in-cylinder gas temperatures. Further investigations, performed adopting 10% EGR for HCNG blends, showed a large reduction of NO_x emission, over 80% compared with natural gas (without EGR), with a positive effect also on engine efficiency. The decrease in fuel consumption using HCNG blends together with EGR, compared with natural gas, was 5.4%, 6.6% and 7.7% for HCNG 10, 20 and 30, respectively.

Copyright © 2011, Hydrogen Energy Publications, LLC. Published by Elsevier Ltd. All rights reserved.

* Corresponding author. Tel.: +39 0815010284; fax: +39 0815010204.

E-mail addresses: antonio.mariani@unina2.it (A. Mariani), biagio.morrone@unina2.it (B. Morrone), andrea.unich@unina2.it (A. Unich).
0360-3199/\$ – see front matter Copyright © 2011, Hydrogen Energy Publications, LLC. Published by Elsevier Ltd. All rights reserved.
doi:10.1016/j.ijhydene.2011.10.082

1. Introduction

Natural gas-hydrogen blends (HCNG) can be a viable alternative to pure fossil fuels because of the expected increase of engine efficiency and the reduction of total pollutant emissions. These blends offer a valid opportunity for dealing with a sustainable development in transportation, in view of the future more stringent emission limits for road vehicles. The problem of pollution is especially felt in great urban areas, where cars and heavy-duty vehicles strongly contribute to total pollutant emissions.

Natural Gas vehicles present lower pollutant and carbon dioxide emissions compared to gasoline vehicles [1]. Moreover, its high anti-knock property value allows increasing the compression ratio, compared with gasoline engines, with positive effects on engine efficiency. However, homogeneous spark-ignited NG engines have lower volumetric efficiency since NG occupies a fraction of intake charge which implies a decrease in fresh air into the cylinder and thus in the output power [2].

Hydrogen can be used as fuel in internal combustion engines. Das et al. [3] compared performance and combustion characteristics of an engine fuelled with both hydrogen and compressed natural gas. They found that brake thermal efficiency improved with hydrogen operation compared to compressed natural gas.

Natural Gas engine performance can be increased by using hydrogen as additive to achieve natural gas-hydrogen blends. In fact, hydrogen addition increases the laminar flame speed of NG, which is lower than gasoline [4], thus increasing engine efficiency.

Raman et al. [5] carried out an experimental study on SI engines fuelled with HCNG blends from 0% to 30% of H₂ in a V8 engine. The authors observed a reduction of NO_x emissions with 15%–20% hydrogen blends with some increase of HC emissions as a result of ultra-lean combustion. Hoekstra et al. [6] observed a reduction of NO_x for hydrogen percentage up to 30%, limit beyond which no improvement was observed. An important point was the higher flame speed and a consequent reduction of the spark advance angle to obtain the maximum brake torque, as already indicated by Nagalingam et al. [7]. Karim et al. [8] published experimental results of a natural gas fuelled internal combustion engine claiming that hydrogen as additive to NG can strongly improve the performance of such engines, especially in terms of power, efficiency and emissions, allowing engine operation with lean mixtures. In addition, hydrogen does not affect the anti-knock performance of NG fuel. Larsen and Wallace [9] accomplished experimental tests on heavy-duty engines fuelled by HCNG blends. The authors found that HCNG blends improve efficiency and reduce CO, CO₂ and HC emissions. Sierens and Rossel [10] determined that the optimal HCNG composition to obtain low HC and NO_x emissions should be varied with engine load.

Huang et al. [11] accomplished an experimental study for a direct-injection spark ignition engine fuelled with HCNG blends under various ignition timings and lean mixture conditions. The ignition timing is an important parameter for improving engine performance and combustion.

Road tests on urban transport buses have been performed by Genovese et al. [12], comparing energy consumption and

exhaust emissions for NG and HCNG blends with hydrogen content between 5% and 25% in volume. The authors found that average engine efficiency over the driving cycle increases with hydrogen content and NO_x emissions were higher for blends with 20% and 25% of hydrogen, despite the lean relative air fuel ratios and delayed ignition timings adopted.

Having reviewed the main experimental papers published in the past, also the numerical analysis plays a fundamental role in research activities, allowing a better design of the experimental tests with cost savings and time reduction.

In 2008, Mariani et al. [13] developed a numerical engine model and carried out an investigation on HCNG blends with hydrogen content up to 30%. The authors stated that by employing MBT spark advance, such HCNG blends exhibit improvements of engine brake efficiency compared with NG, which are more relevant at part loads and for the highest hydrogen content. NO_x emissions were reduced by means of exhaust gas recirculation.

Morrone and Unich carried out a numerical investigation on the characteristics of natural gas-hydrogen blends as well as their effect on engine performance [14]. Results showed an increase in engine efficiency only if MBT spark advance is used for each fuel. Moreover, the authors performed an economic analysis and determined the over cost of hydrogen in such blends, showing percent increments between 6 and 30% for different hydrogen content.

The prediction of CO and NO_x emissions has been carried out by Tinaut et al. [15] adopting the thermo-chemical models, considering four different proportions of hydrogen and NG (up to 15% of hydrogen in volume) with an equivalence ratio of 0.8. CO emissions were slightly influenced by hydrogen addition as a consequence of the lean combustion conditions. When the percentage of hydrogen raised, the NO emissions increased. Maximum NO emissions were reached for an engine speed of 2400 rpm. The model could also predict the indicated engine efficiency which raised as the percentage of hydrogen increased. Park et al. [16] performed a numerical analysis to investigate the performance and emission characteristics of an engine fuelled by methane and methane-hydrogen blends at lean operating conditions obtaining an engine efficiency increase of 7% when a 15% hydrogen content was adopted.

In this paper a numerical model of an internal combustion spark ignition engine fuelled by natural gas and hydrogen-natural gas blends, HCNG 10, HCNG 20 and HCNG 30, has been developed. Simulations were performed at conditions reproducing engine operation on a passenger car over NEDC. Stoichiometric air-to-fuel ratio was considered for each fuel in order to assure an efficient exhaust after-treatment adopting a three-way catalyst. Exhaust gas recirculation was investigated with the aim at improving engine efficiency and reducing NO_x emissions [17]. In fact, HCNG blends combustion properties are particularly suitable for EGR, assuring a stable combustion also if the charge is diluted [18]. MBT ignition timing has been adopted for all fuels and operating conditions investigated.

The results showed that HCNG blends improved engine brake efficiency, particularly at low loads and for the highest hydrogen content, with fuel consumptions on energy basis

over NEDC 2.5%, 4.7% and 5.7% lower than CNG, for HCNG 10, 20 and 30 respectively. NOx emissions increased of about 4% for HCNG 10, 11% for HCNG 20 and 19.7% for HCNG 30, due to the higher gas temperatures. A large reduction of such pollutant and a further increase of engine efficiency were achieved by using 10% EGR. Indeed, the mixture dilution decreases the combustion temperature and consequently the NOx formation. The results showed reductions of such pollutant greater than 80% compared with natural gas (without EGR) for all the HCNG blends. The reduction in fuel consumption (MJ/km) for the HCNG blends with EGR respect to CNG was found to be between 5% and 8%.

2. Numerical model

2.1. Engine model

The numerical engine model has been developed using a one dimensional discretization for pipes whereas, inside the cylinders, a zero dimensional model has been adopted. The intake and exhaust pipes, together with a muffler, were divided into small volumes. The cells are connected to each other through boundaries, where the vector variables are calculated. Instead, the scalar variables, such as temperature, pressure, enthalpy, density and species concentration are evaluated at the center of each cell volume. The differential equations solved are:

1. Mass conservation
2. Momentum equation
3. Energy equation

The solution has been obtained by integrating the above described equations explicitly in time and the time step automatically adapts to satisfy the CFL limit [19]. The length of discretization has been chosen equal to 0.4 times the cylinder bore for intake and 0.5 for the exhaust pipe.

The analysis of the combustion process was carried out by considering a two-zone model [20]. This model divides the cylinder volume into burned and unburned zones and considers the flame front of zero thickness [21]. The model is made up of the energy equations for the unburned (u) and burned (b) zones, mass conservation, a volume conservation equation and two ideal gas equations:

$$\frac{d(m_k e_k)}{dt} = -p \frac{dV_k}{dt} - \dot{Q}_k - \left(h_f \frac{dm_f}{dt} + h_a \frac{dm_a}{dt} \right) \quad k = u, b \quad (1)$$

$$m_u + m_b = m \quad (2)$$

$$V_u + V_b = V \quad (3)$$

where m_k is the total mass inside the considered zone, m_a the air mass, m_f the fuel mass, e_k the total internal energy, p the cylinder pressure, V_k the volume, \dot{Q}_k the heat transfer rate across the cylinder walls, h_f the fuel enthalpy, h_a the air enthalpy, and u and b indexes refer to unburned and burned zone, respectively.

Table 1 – Engine characteristics.

Engine type	4 cylinder, SI
Displacement	1242 cm ³
Bore × Stroke	70.8 × 78.86 mm
Compression ratio	9.8:1
Rated Power	38 kW at 5000 rpm

The pressure is assumed uniform inside the cylinder, thus for the two zones it holds:

$$p = \frac{m_b R_b T_b}{V_b} = \frac{m_u R_u T_u}{V_u} \quad (4)$$

The model calculates the combustion speed from the laminar combustion velocity S_L :

$$S_L = \frac{dm_b}{A_f dt} \quad (5)$$

where A_f is the flame front area and ρ_u the density of the unburned region gas. An experimental correlation between laminar flame speed and engine operating parameters is expressed by Equation (6), [20]:

$$S_L = \left(B_{\max} + B_\phi (\phi - \phi_m)^2 \right) \left(\frac{T_u}{T_0} \right)^\delta \left(\frac{p}{p_0} \right)^\beta (1 - 2.06 \cdot y_{\text{dil}}^{0.77}) \quad (6)$$

where B_{\max} is the maximum laminar speed, B_ϕ a coefficient, ϕ and ϕ_m are the actual and maximum flame speed equivalence ratio respectively, y_{dil} is the molar fraction of burned gas inside the cylinder, and δ and β are coefficients which take into account the effects of temperature and pressure.

The burn rate x_b is defined as:

$$\frac{dx_b}{d\theta} = \frac{d}{d\theta} \left(\frac{m_{f,b}}{m_{f,T}} \right) \quad (7)$$

where $m_{f,b}$ is the burned fuel mass, $m_{f,T}$ is the total fuel mass and θ is the crank angle. Burn rate is predicted considering the turbulent integral scale, the turbulent micro-scale, the turbulent intensity, and the laminar flame speed [21–23]. The effects of major in-cylinder fluid motions have been considered [24].

The model allows the determination of the engine actual cycle and hence, after the estimation of friction losses, the computation of engine brake efficiency, which is defined as:

$$\eta_{br} = \frac{P_{sh}}{\dot{m}_f LHV} \quad (8)$$

Table 2 – Properties of Natural Gas (CNG) and hydrogen – natural gas blends (HCNG).

	CNG	HCNG 10	HCNG 20	HCNG 30
H ₂ [% vol]	–	10	20	30
H ₂ [% energy]	–	3.17	7.02	11.8
LHV _m [MJ/kg]	45.3	46.2	47.3	48.6
LHV _v [MJ/Nm ³]	36.9	34.3	31.7	29.0
LHV _v Stoich. mix [MJ/Nm ³]	3.37	3.37	3.36	3.35
α_{stoic} [kg _{air} /kg _{fuel}]	15.6	15.8	16.1	16.4
S_L at α_{stoic} [m/s]	0.35	0.38	0.41	0.44

Table 3 – Vehicle characteristics used for engine torque and speed determination.

Mass [kg]	1025
Frontal area [m ²]	1.97
Rolling resistance coefficient	0.013
Aerodynamic resistance coefficient	0.3
Transmission efficiency	0.95
Wheel radius [m]	0.293
Gear	Total Transmission ratio
I	13.4
II	7.42
III	5.09
IV	3.85
V	3.08

with P_{sh} the mechanical power delivered at the shaft, \dot{m}_f the fuel mass flow rate and LHV the lower heating value of the fuel.

The nitric oxide formation is modelled using the extended Zeldovich mechanism [25], described by the following chemical relations:



The main characteristics of the investigated engine are reported in Table 1.

Stoichiometric air-to-fuel ratio was considered for each fuel in order to assure an efficient exhaust after-treatment adopting a three-way catalyst. Exhaust gas recirculation was investigated (instead of ultra-lean mixture) with the aim at improving engine efficiency and reducing NOx emissions. In fact, HCNG blends combustion properties are particularly suitable for EGR, assuring a stable combustion also if the charge is diluted. MBT ignition timing has been adopted for all fuels and operating conditions investigated.

The properties of the fuels are reported in Table 2. The lower heating value on mass basis LHV_m increases with H₂ content, whereas the LHV_v , referred to the volume, decreases with increasing hydrogen content, due to its very low density. Since hydrogen burning velocity is about eight times higher than the methane one at stoichiometric conditions [26], the laminar flame speed of the blends increases with hydrogen content [27,28].

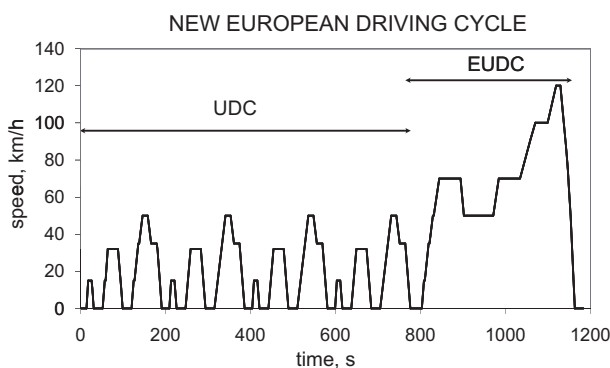


Fig. 1 – New European Driving Cycle (NEDC) speed profile as a function of the time.

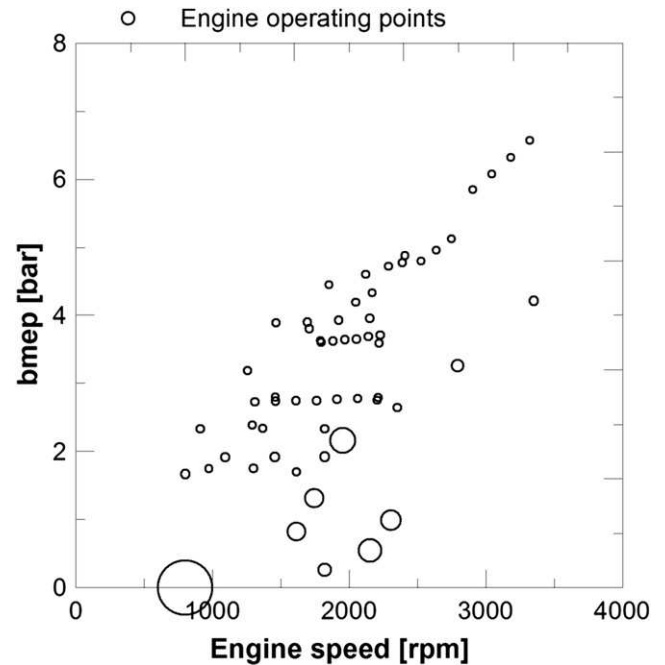


Fig. 2 – Engine operating points for the NEDC.

2.2. Determination of the operating points

Vehicle characteristics, reported in Table 3, allowed identifying engine operating conditions during New European Driving Cycle, Fig. 1.

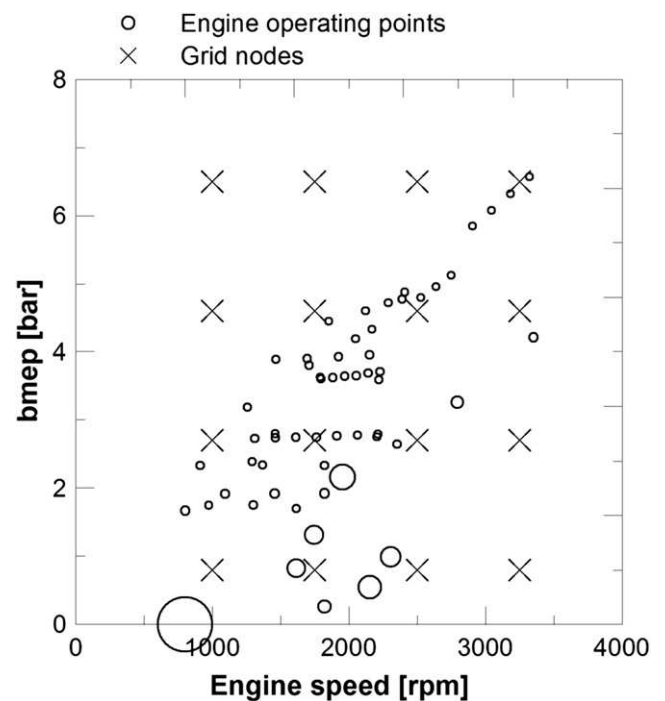


Fig. 3 – Engine operating points and grid nodes used for the numerical analysis.

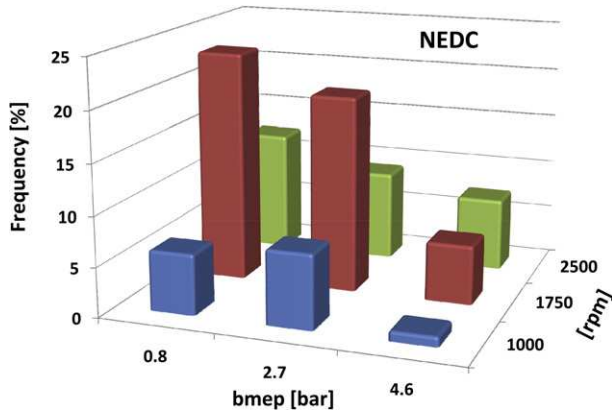


Fig. 4 – Frequency distribution of operating points for the NEDC.

As driving cycle and vehicle characteristics are known, vehicle traction force can be determined by means of the equation of longitudinal dynamics:

$$F_t = m \frac{dv}{dt} + [F_a + F_r + F_g] \quad (10)$$

being $m(dv/dt)$ the inertia force of the vehicle, F_a the aerodynamic resistance, F_r the rolling resistance and F_g the gravity force component along the motion direction [29]. A time step of 1 s has been considered to solve Equation (10).

Once F_t is known, vehicle characteristics allow calculating engine torque and speed for each time step and then brake mean effective pressure (bmep), defined as:

$$\text{bmep} = \frac{C \cdot 4\pi}{V_d} \quad (11)$$

where C is the torque and V_d is the displacement.

Brake mean effective pressure versus engine speed is displayed in Fig. 2, where each circle represents an engine operating point which radius is proportional to the time spent at such condition. It can be observed that, during the NEDC, the engine is frequently run in small portions of the plane.

In order to reduce the number of simulations, a limited number of operating conditions has been considered by placing 16 points equally spaced on the bmep – engine speed plane, Fig. 3.

Each couple of bmep and engine speed values previously calculated is then attributed to the adjacent points of the grid by using the following criterion:

$$\sum_{i=1}^m C_i \cdot \omega_i \cdot t_i = C \cdot \omega \cdot t \quad (12)$$

being ω the engine speed and t the time step of the driving cycle simulation; C_i , ω_i and t_i are the torque, the engine speed and residence time of the i -th node respectively, where t_i is determined as follows:

$$t_i \propto \frac{1}{S_i} \quad (13)$$

being S_i the distance from the operating point and the i -th grid node [30]. The Equation (13) does not apply when the

operating point coincides with one of the grid nodes. Hence, total residence time is calculated for each grid node.

The frequency distribution of the residence time at each node, reported in Fig. 4, shows the preponderance of operating points with low bmep and intermediate speeds.

Once fuel and NOx mass flow rates are estimated by the engine model at each point of the grid, such values are multiplied for the residence time, obtaining the total fuel mass consumption and NOx emissions on the whole cycle.

Anyway, such approach does not take into account the effects of thermal and load transients, which can affect NOx emissions.

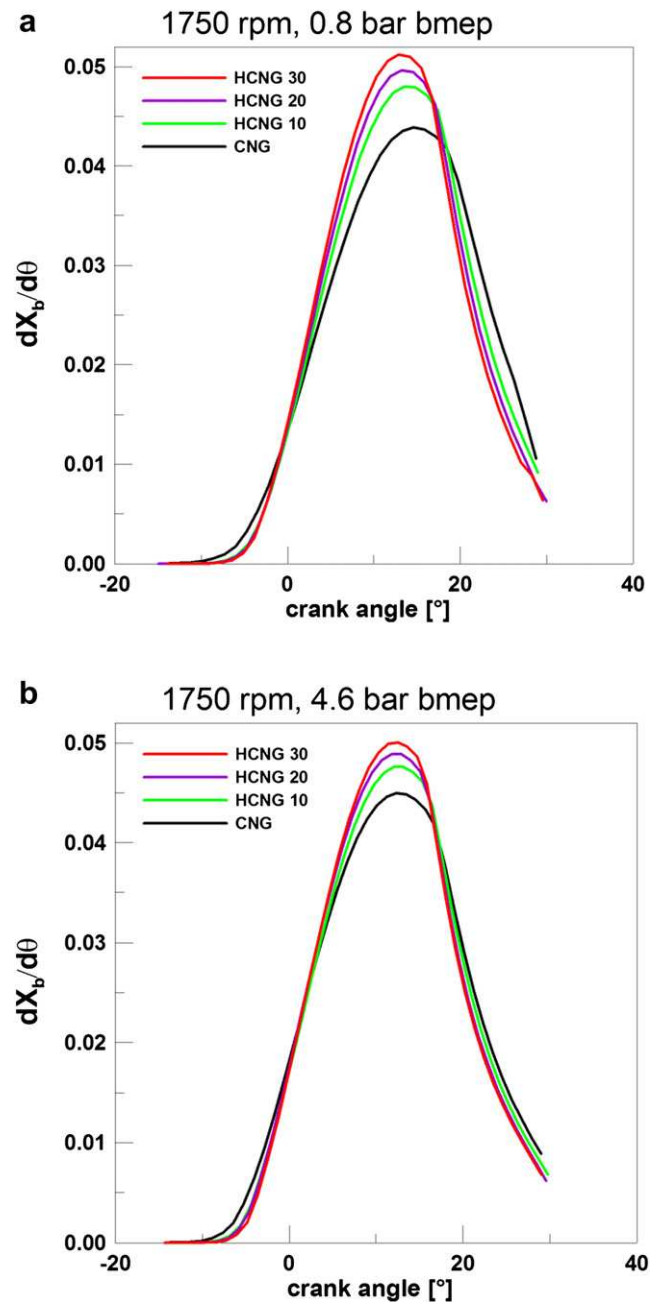


Fig. 5 – Normalized Burn Rate as a function of crank angle: (a) 0.8 bar bmep and 1750 rpm; (b) 4.6 bar bmep and 1750 rpm.

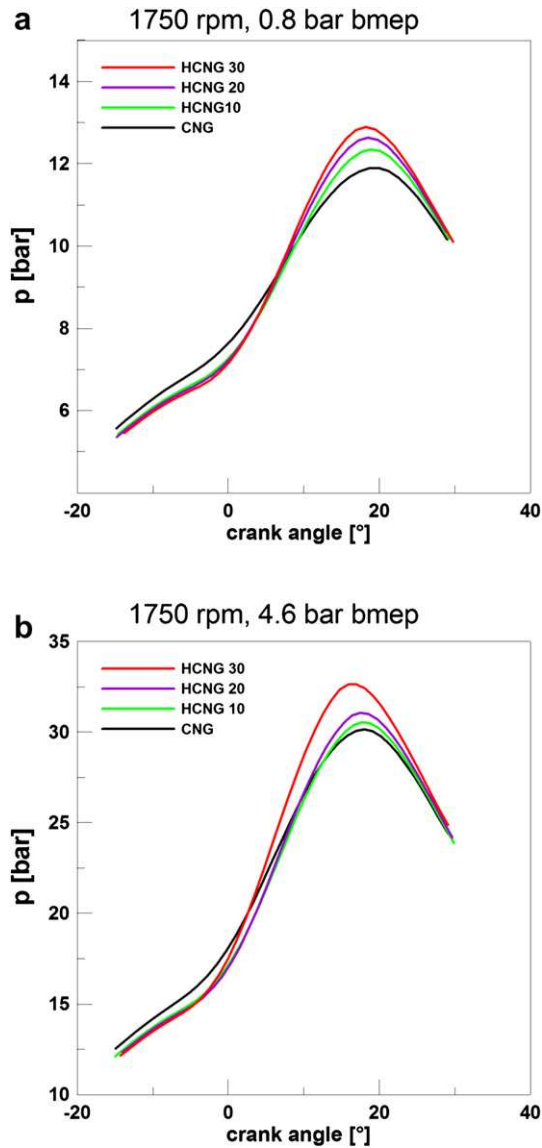


Fig. 6 – Cylinder pressure as a function of crank angle: (a) 0.8 bar bmep and 1750 rpm; (b) 4.6 bar bmep and 1750 rpm.

3. Results and discussion

Fig. 5 shows that HCNG blends present a higher burn rate than CNG, which increases with hydrogen content. The increment of burn rate peak is about 9% when comparing CNG and HCNG 10 fuels at 0.8 bar bmep, Fig. 5(a). Further increases, 13% and 17%, are attained with HCNG 20 and 30, respectively. At 4.6 bar bmep, burn peak rates 6%, 9% and 11% larger than natural gas are obtained for HCNG 10, 20 and 30 respectively, Fig. 5(b). Hydrogen addition reduces the effects of residual gases on combustion speed, in particular at low loads, when residual gas fraction is high.

As the burn rate increases due to hydrogen addition, higher cylinder pressures are attained in the combustion chamber, as shown in Fig. 6. Fig. 6(a) shows larger peak pressure values than natural gas of 4% for HCNG 10, 6% for HCNG 20 and 8% for HCNG 30 at 0.8 bar bmep, while Fig. 6(b), at 4.6 bar bmep,

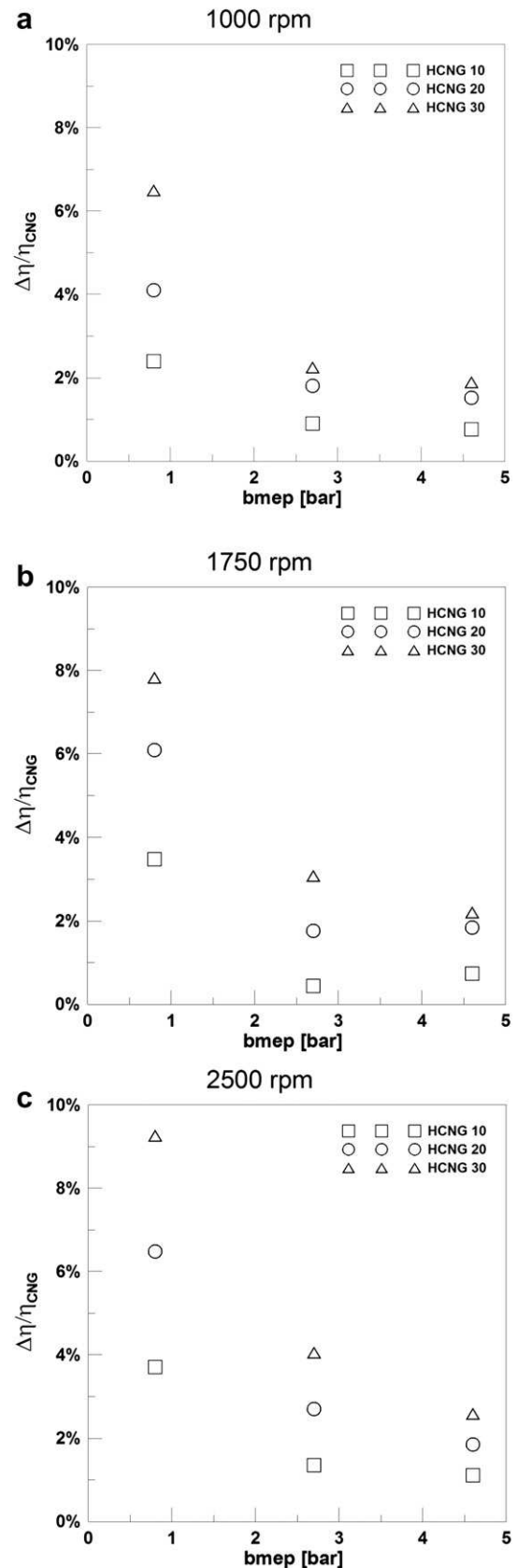


Fig. 7 – Percent increment of engine brake efficiency as a function of bmep; (a) 1000 rpm; (b) 1750 rpm; (c) 2500 rpm.

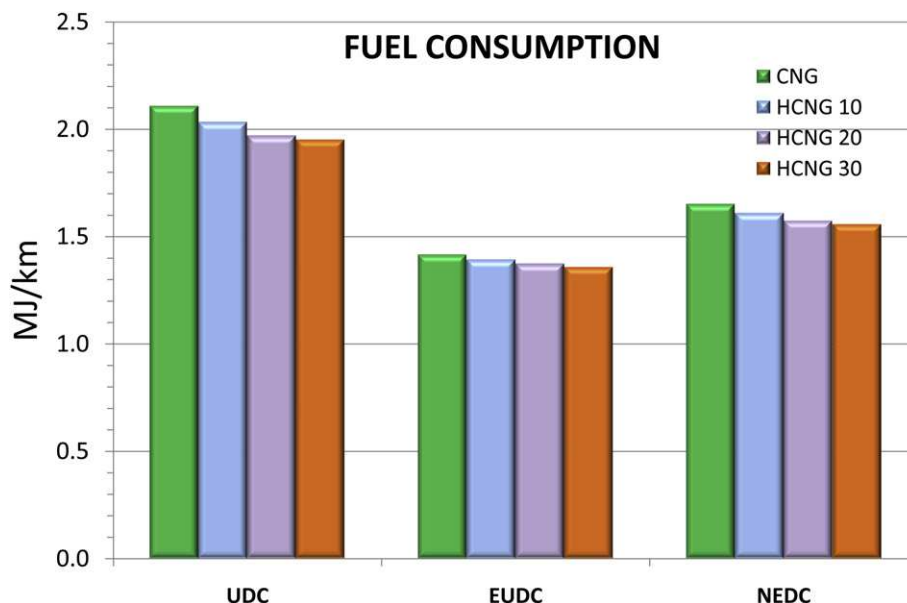


Fig. 8 – Fuel consumption in MJ/km over the urban (UDC), the extra-urban (EUDC) and the NEDC cycles.

shows 1% increments for HCNG 10, 3% for HCNG 20, and 8% for HCNG 30. Maximum cylinder pressure is located nearly at the same crank angle as a result of optimized ignition timing.

Fig. 7 shows the effect of the blends on engine brake efficiency, which increases with hydrogen content as a consequence of a higher burning speed promoted by hydrogen. The increments are higher at low engine loads and high speeds, with improvements of 3.7% for HCNG 10, 6.5% for HCNG 20 and 9.3% for HCNG 30, at 0.8 bar bmep and 2500 rpm, Fig. 7(c).

Fig. 8 shows the prediction of fuel consumption in terms of energy per kilometer over the urban (UDC), the extra-urban (EUDC) and the NEDC cycles for CNG, HCNG 10, HCNG 20 and HCNG 30. The fuel consumption reduction ranges between 3.4% and 7.4% over UDC, between 1.6% and 4.1% over

the EUDC and between 2.5% and 5.7% over the NEDC, with the values referred to HCNG 10 and 30 respectively. The positive effects of hydrogen addition are more evident over the urban part of the driving cycle where the engine operates mainly at low loads, with the most representative operating condition being at 0.8 bar bmep and 1750 rpm. Over the EUDC, a lower increase on engine efficiency is attained because the engine operates mainly at medium load, with the longest residence time located at 2.7 bar bmep and 1750 rpm.

The NO_x emissions, expressed in g/km over the driving cycles, are reported in Fig. 9. Using HCNG blends higher in-cylinder temperatures are attained as a consequence of a faster combustion, resulting in increased NO_x emissions. This behaviour is observed over all the considered driving

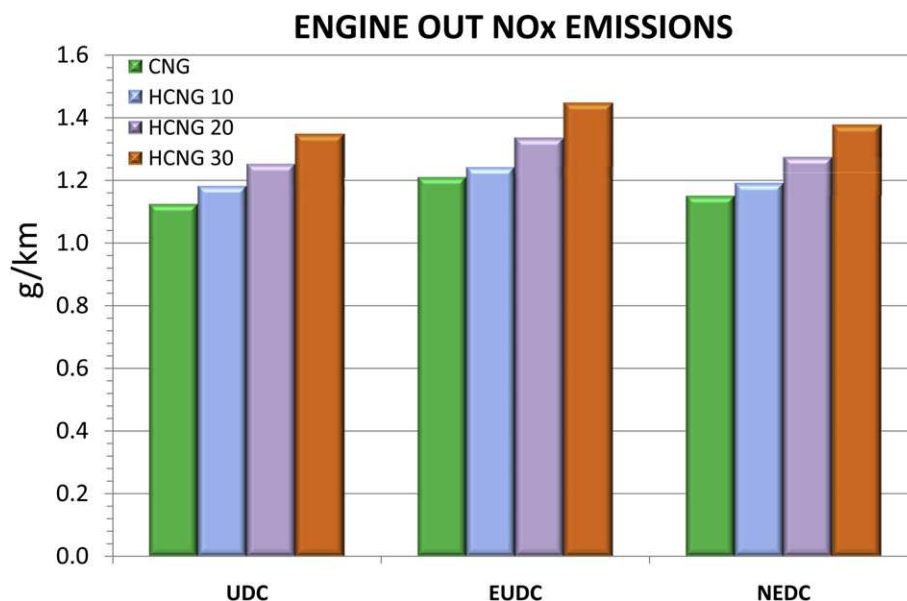


Fig. 9 – NO_x emissions over the UDC, EUDC and NEDC.

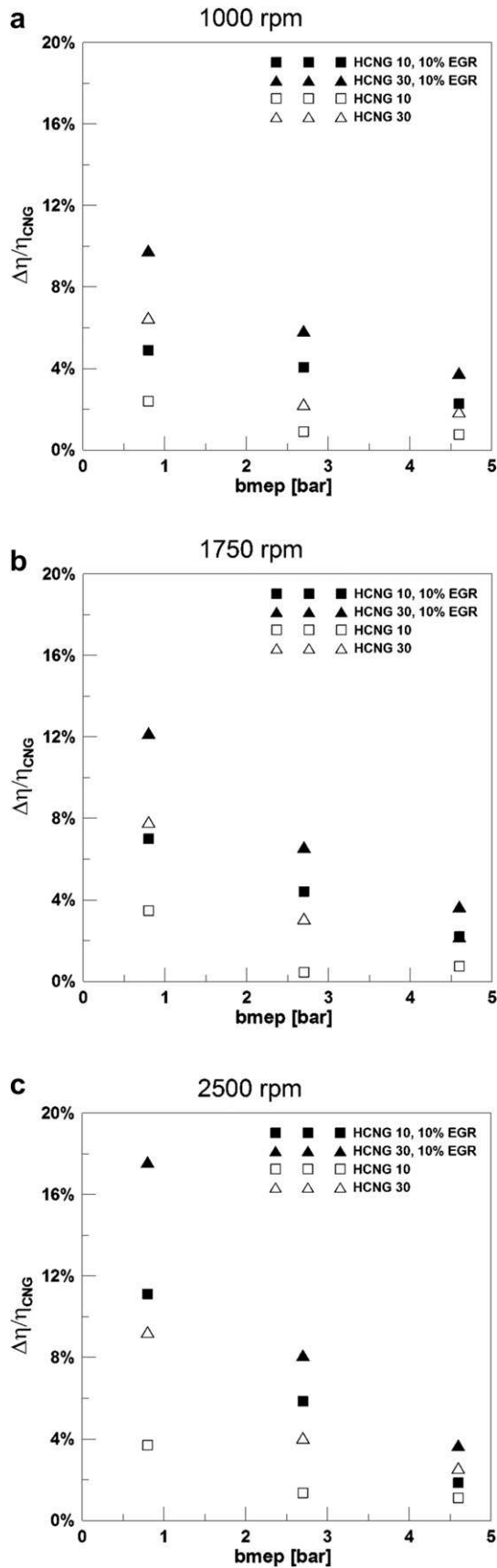


Fig. 10 – Percent increment of engine brake efficiency as a function of the bmep, (a) 1000 rpm; (b) 1750 rpm; (c) 2500 rpm.

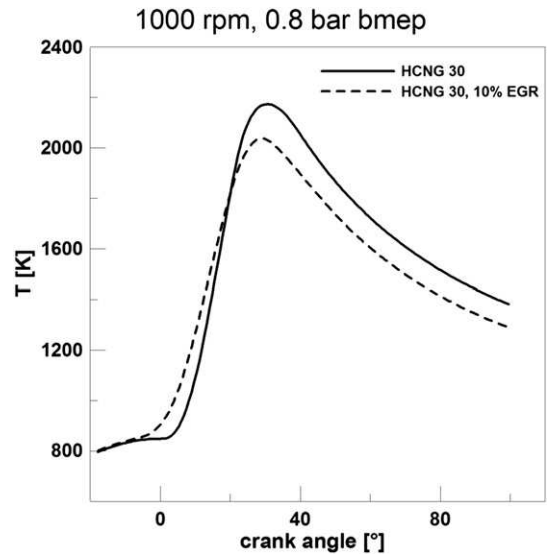


Fig. 11 – In-cylinder gas temperature versus crank angle for HCNG 30 at 1000 rpm and 0.8 bar bmep.

cycles, with higher increases over the UDC with values of 5% for HCNG 10, 11% for HCNG 20 and 20% for HCNG 30. Over the EUDC emissions increased of 2.6% for HCNG 10, 10% for HCNG 20 and 20% for HCNG 30.

Since HCNG blends are suitable to be used with lean mixtures or high residual gas fraction keeping a good combustion stability, the exhaust gas recirculation has been adopted with the aim at increasing engine efficiency and reducing NOx emissions, retaining a stoichiometric air-to-fuel ratio. The following results have been obtained using 10% EGR.

Fig. 10 shows the variation of brake efficiency for the blends with and without EGR with respect to natural gas.

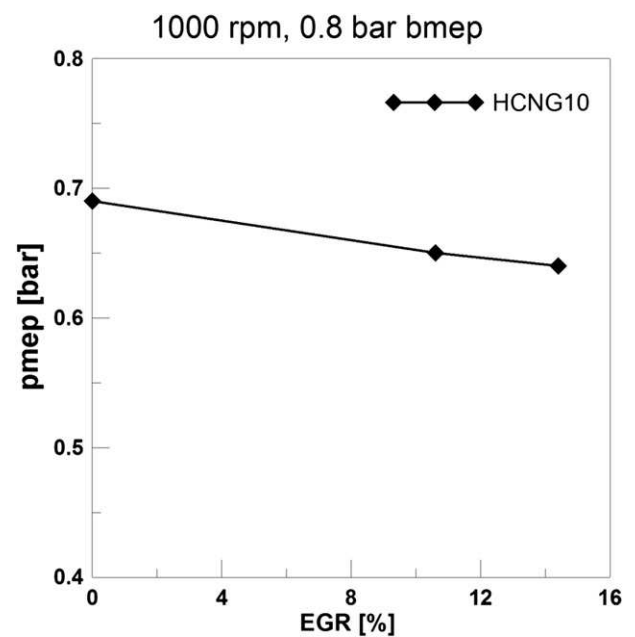


Fig. 12 – Pumping Mean Effective Pressure (p_{mep}) versus EGR rate for HCNG 10 at 1000 rpm and 0.8 bar bmep.

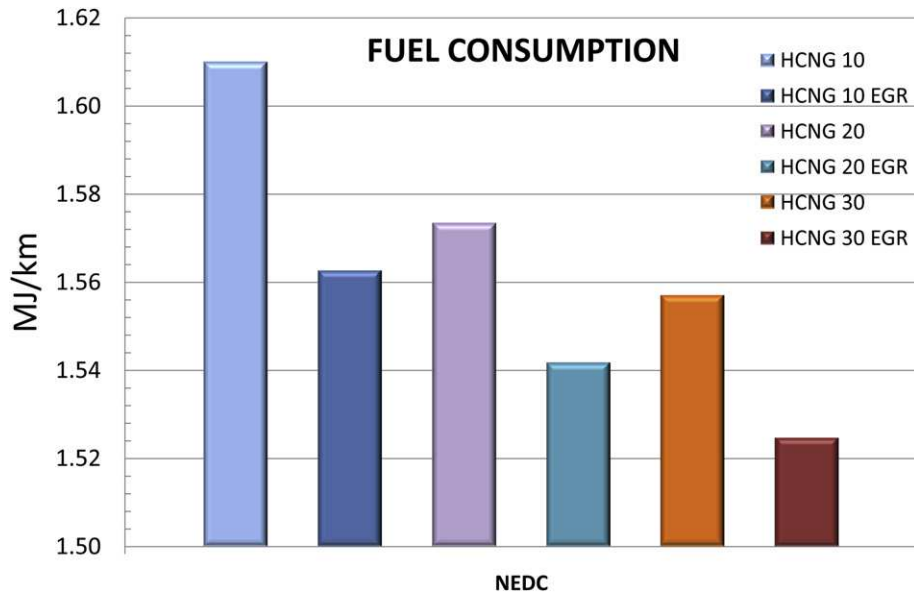


Fig. 13 – Fuel consumption in MJ/km over the EUDC, for HCNG 10, 20 and 30 with 10% EGR and without EGR.

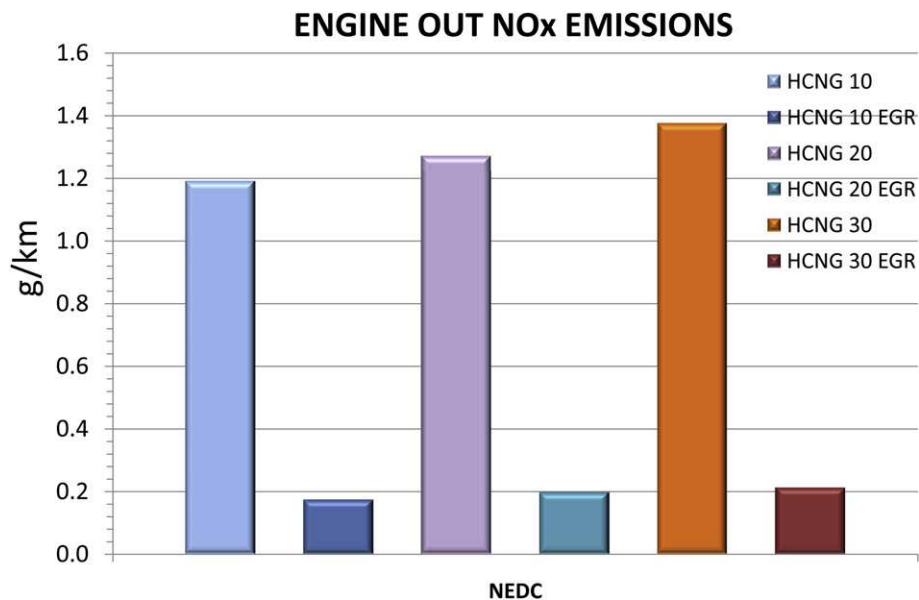


Fig. 14 – Comparison of NOx emissions over the NEDC for HCNG blends with 10% EGR and without EGR.

Nevertheless the increases in engine efficiency of HCNG blends with exhaust gas recirculation were higher than those obtained without EGR, with a maximum of 17.6% for HCNG 30 at 0.8 bar bmep and 2500 rpm. The positive effect of EGR on engine brake efficiency is the consequence of lower temperature attained in the combustion chamber, as shown in Fig. 11, with reduced burned gases dissociation and decreased heat loss to the walls. Furthermore EGR reduced pumping work at constant bmep, as shown in Fig. 12 as an example for the operating condition of 1000 rpm and 0.8 bar bmep.

The higher engine efficiencies attained with EGR reduce further fuel consumption, Fig. 13. The reduction, calculated with respect to natural gas, ranges between 6.4% and 8.7%

over the UDC, 4.3% and 6.6% over the EUDC which brings decrease between 5.4% and 7.7% over the NEDC, with the values referred to HCNG 10 and HCNG 30, respectively.

The use of EGR results in lower NOx emissions with respect to the case without EGR as shown in Fig. 14, with values about 85% lower than CNG for each HCNG fuel.

4. Conclusions

A numerical engine model has been developed to predict fuel consumption and NOx emissions of a spark ignition engine fuelled with natural gas and hydrogen – natural gas blends

over the NEDC. The results display the impact of the increased fuel burn rate due to hydrogen addition.

Simulations were performed at conditions reproducing engine operation on a passenger car over NEDC. Stoichiometric air-to-fuel ratio was considered for each fuel. Exhaust gas recirculation was investigated with the aim at improving engine efficiency and reducing NOx emissions. MBT ignition timing has been adopted for all fuels and operating conditions investigated.

The following results display the variations of fuel consumption and NOx emissions of HCNG blends respect to natural gas, over the driving cycle:

1. HCNG blends improved engine brake efficiency, in particular at low loads and for the highest hydrogen content. These effects produced a reduction in fuel consumption, expressed in MJ/km, over the NEDC of 2.5%, 4.7% and 5.7% compared to natural gas for HCNG blends with 10%, 20% and 30% of hydrogen, respectively.
2. NOx emissions increased of about 4% for HCNG 10, 11% for HCNG 20 and 20% for HCNG 30, due to higher temperatures into the cylinders than those attained with natural gas.
3. The use of EGR implied a reduction of NOx emissions for HCNG blends with respect to natural gas (without EGR) larger than 80%.
4. Furthermore, augmentation in engine efficiency was obtained using EGR due to reduced burned gases dissociation and reduced heat losses to the walls because of the lower in-cylinder temperatures attained. The reductions in fuel consumption with HCNG blends and EGR, compared with natural gas, were 5.4%, 6.6% and 7.7% for HCNG 10, 20 and 30 respectively.

Acknowledgements

This work has been supported by a PRIST 2008 grant by the Seconda Università degli studi di Napoli, together with a 2011 research grant funded by the Seconda Università degli studi di Napoli.

Nomenclature

A	Area, m ²
bme _p	Brake mean effective pressure, Pa
B _{max}	Maximum flame speed, m/s
B _φ	Numerical coefficient
C	Torque, N m
CFL	Courant-Friedrichs-Lewy
e	Energy, MJ/kg
EGR	Exhaust Gas Recirculation
F _a	Aerodynamic resistance, N
F _r	Rolling resistance, N
F _g	Gravity force component in motion direction, N
F _t	Traction force, N
h	Enthalpy, kJ/kg
MBT	Maximum Brake Torque

LHV	Lower Heating Value, MJ/kg or MJ/Nm ³
m	Mass, kg
\dot{m}	Mass flow rate, kg/s
NOx	Nitrogen oxides
p	Pressure, bar
P _{sh}	Shaft Engine Power, kW
\dot{Q}	Heat rate, kW
R	Gas constant, kJ/kg K
S _L	Flame speed, m/s
s	Grid node distance from operating points, –
SI	Spark ignition
T	Temperature, K
t	Time, s
V	Volume, m ³
v	Speed, m/s
x _b	Burned mass fraction, –
y _{dil}	Dilution mole fraction, –

Greek symbols

α	Air-to-fuel ratio, kg _{air} /kg _{fuel}
δ	Temperature power exponent
β	Pressure power exponent
θ	Crank Angle, °
η	Efficiency, –
φ	Equivalence ratio, –
ρ	Density, kg/m ³
ω	Engine speed, rad/s

Subscripts

air	Air
b	Burned
br	Brake
d	Displacement
f	Fuel
m	Mass
i	i-th node
stoic	Stoichiometric
u	Unburned
V	Volume
0	Reference

REFERENCES

- [1] Ristovski Z, Morawska L, Ayoko GA, Johnson G, Gilbert D, Greenaway C. Emissions from a vehicle fitted to operate on either petrol or compressed natural gas. *Sci Total Environ* 2004;323:179–94.
- [2] Mello P, Pelliza G, Cataluna R, da Silva R. Evaluation of the maximum horsepower of vehicles converted for use with natural gas fuel. *Fuel* 2006;85:2180–6.
- [3] Das LM, Gulati R, Gupta PK. A comparative evaluation of the performance characteristics of a spark ignition engine using hydrogen and compressed natural gas as alternative fuels. *Int J Hydrogen Energy* 2000;25:783–93.
- [4] Karim GA. Hydrogen as a spark ignition engine fuel. *Int J Hydrogen Energy* 2003;28:569–77. Elsevier.
- [5] Raman V, Hansel J, Fulton J, Lynch F, Bruderly D. Hythane - an ultraclean transportation fuel. *Procs. of 10th World Hydrogen Conference, Cocoa Beach, Florida, USA, 1994.*

- [6] Hoekstra RL, Collier K, Mulligan N, Chew L. Experimental study of a clean burning vehicle fuel. *Int J Hydrogen Energy* 1995;20:737–45.
- [7] Nagalingam B, Duebel F, Schmillen K. Performance study using natural gas, hydrogen-supplemented natural gas and hydrogen in AVL research engine. *Int J Hydrogen Energy* 1983;8:715–20.
- [8] Karim GA, Wierzbka I, Al-Alousi Y. Methane-Hydrogen mixtures as fuels. *Int J Hydrogen Energy* 1996;21:625–31.
- [9] Larsen JF, Wallace JS. Comparison of emissions and efficiency of a turbocharged lean-burn natural gas and hythane-fueled engine. *J Eng for Gas Turbines Power* 1997;119:218–26.
- [10] Sierens R, Rosseel E. Variable composition Hydrogen/Natural gas mixtures for increased engine efficiency and decreased emissions. *J Eng for Gas Turbines Power* 2000;122:135–40.
- [11] Huang Z, Wang J, Liu B, Zeng K, Yu K, Jiang D. Combustion characteristics of a direct-injection engine fueled with natural gas-hydrogen blends under different ignition timings. *Fuel* 2007;86:381–7.
- [12] Genovese A, Contrisciani N, Ortenzi F, Cazzola V. On road experimental tests of hydrogen/natural gas blends on transit buses. *Int J Hydrogen Energy* 2011;36:1775–83.
- [13] Mariani A, Morrone B, Unich A. Numerical modelling of internal combustion engines fuelled by hydrogen-natural gas blends. *ASME Int Mech Eng Congress Exposition*; 2008.
- [14] Morrone B, Unich A. Numerical investigation on the effects of natural gas and hydrogen blends on engine combustion. *Int J Hydrogen Energy* 2009;33:4626–34.
- [15] Tinaut FV, Melgar A, Giménez B, Reyes M. Prediction of performance and emissions of an engine fuelled with natural gas/hydrogen blends. *Int J Hydrogen Energy* 2011;36:947–56.
- [16] Park J, Cha H, Song S, Min Chun K. A numerical study of a methane-fueled gas engine generator with addition of hydrogen using cycle simulation and DOE method. *Int J Hydrogen Energy* 2011;36:5153–62.
- [17] Hu E, Huang Z, Liu B, Zheng J, Gu X, Huang B. Experimental investigation on performance and emissions of a spark-ignition engine fuelled with natural gas hydrogen blends combined with EGR. *Int J Hydrogen Energy* 2009;34:528–39.
- [18] Hu E, Huang Z, Liu B, Zheng J, Gu X. Experimental study on combustion characteristics of a spark-ignition engine fueled with natural gas–hydrogen blends combining with EGR. *Int J Hydrogen Energy* 2009;34:1035–44.
- [19] Courant R, Friedrichs K, Lewy. On the partial difference equations of mathematical physics. *IBM J* 1967;11:215–34.
- [20] Heywood JB. *Internal combustion engine fundamentals*. New York: McGraw-Hill; 1988.
- [21] Borman GL, Ragland KW. *Combustion engineering*. Boston: McGraw-Hill; 1998.
- [22] Hires SD, Tabaczynski RJ, Novak JM. The prediction of ignition delay and combustion intervals for a homogeneous charge spark ignition engine. *SAE Paper*; 1978. 780232.
- [23] Blizard NC, Keck JC. Experimental and theoretical investigation of turbulent burning model for internal combustion engine. *SAE Paper*; 1974. 740191.
- [24] Morel T, Rackmil CI, Keribar R, Jennings MJ. Model for heat transfer and combustion in spark-ignited engine and its comparison with experiments. *SAE Paper*; 1988. 880198.
- [25] Glassman I, Yetter RA. *Combustion*. New York: Academic Press Elsevier; 2008.
- [26] Ilbas M, Crayford AP, Yilmaz I, Bowen PJ, Syred N. Laminar-burning velocities of hydrogen–air and hydrogen–methane–air mixtures: an experimental study. *Int J Hydrogen Energy* 2006;31:1768–79.
- [27] Halter F, Chauveau C, Djebaili-Chaumeix N, Gokalp I. Characterization of the effects of pressure and hydrogen concentration on laminar burning velocities of methane–hydrogen–air mixtures. *Proc Combust Inst* 2005; 30:201–8.
- [28] Mandilas C, Ormsby MP, Sheppard CGW, Woolley R. Effects of hydrogen addition on laminar and turbulent premixed methane and iso-octane–air flames. *Proc Combust Inst* 2007; 31:1443–50.
- [29] Guzzella L, Sciarretta A. *Vehicle propulsion systems introduction to modelling and optimization*. New York: Springer; 2005. pp. 13–21.
- [30] Gambino M, Iannaccone S, Prati MV, Unich A. Regulated and unregulated emissions reduction with Retrofit catalytic after-treatment on small two Stroke S.I. Engine. *SAE Int Spring Fuels Lubricants Meet Exposition*; 2000. SAE Paper number: 2000-01-1846.